

Partial density of states in the CuInSe_2 valence bands

Cite as: Journal of Applied Physics **81**, 7806 (1997); <https://doi.org/10.1063/1.365390>

Submitted: 23 January 1997 • Accepted: 24 March 1997 • Published Online: 04 June 1998

T. Löher, A. Klein, C. Pettenkofer, et al.



View Online



Export Citation

ARTICLES YOU MAY BE INTERESTED IN

Experimental determination of the N-*p*-partial density of states in the conduction band of GaN: Determination of the polytype fractions in mixed phase samples

Journal of Applied Physics **83**, 1437 (1998); <https://doi.org/10.1063/1.366905>

Light- and bias-induced metastabilities in Cu(In, Ga)Se_2 based solar cells caused by the $(V_{\text{Se}}-V_{\text{Cu}})$ vacancy complex

Journal of Applied Physics **100**, 113725 (2006); <https://doi.org/10.1063/1.2388256>

Hybrid functionals based on a screened Coulomb potential

The Journal of Chemical Physics **118**, 8207 (2003); <https://doi.org/10.1063/1.1564060>



Webinar
Quantum Material Characterization
for Streamlined Qubit Development



Register now

Partial density of states in the CuInSe₂ valence bands

T. Löher, A. Klein, C. Pettenkofer, and W. Jaegermann^{a)}
Hahn-Meiner-Institut, Abteilung CG, Glienicker Strasse 100, 14109 Berlin, Germany

(Received 23 January 1997; accepted for publication 24 March 1997)

The valence band spectra of a vacuum cleaved CuInSe₂(011) surface were measured with synchrotron radiation at photon energies between 16 and 95 eV. The strong dependence of the photoionization cross section of atomic levels between 28 and 60 eV is used to divide the valence band emissions into contributions from Se 4p and Cu 3d states in order to map the respective partial density of states. The derived partial density of Cu 3d states to the total valence band density of states is around 50% in the upper part of the valence band and about 75% at its maximum corresponding to non-bonding Cu d states. © 1997 American Institute of Physics.
[S0021-8979(97)00212-0]

I. INTRODUCTION

The chalcopyrite semiconductors of types I–III–VI₂ are the ternary analogs of the II–VI binary compound semiconductors. The chalcopyrite crystal structure, $\bar{I}4_2m$, is a superlattice of the zinc blende structure, $F\bar{4}3m$, with a nearly doubled *c* axis. The lowest optical gap of the chalcopyrites, however, is considerably smaller than that of the related II–VI analogs, e.g., $E_g(\text{CuInSe}_2) = 1.05$ eV and $E_g(\text{CdSe}) = 1.7$ eV. The band gap reduction is mainly attributed to the hybridization of noble metal *d* states in the upper part of the valence bands which are derived from the chalcogen *p* states.¹ A number of experimental and theoretical studies has therefore been undertaken to derive the partial density of noble metal *d* states at the top of the valence bands.^{1–5} The experimental and theoretical results, however, do not agree; for example in CuInS₂ Cu 3d contributions of 45% (electroreflectance) and 60% (photoemission) were found experimentally and contrasted 24% from the band structure calculation. Respective data for CuInSe₂ are 34% (electroreflectance) and 22% (band structure calculation).

Photoionization cross sections of atomic levels depend in a distinct manner upon the excitation energy. Cross sections of atomic levels over a wide photon energy range have been calculated.⁶ The cross sections of chalcogen *p* states decrease by an order of magnitude by increasing the excitation energy from 20 to 50 eV. By contrast the cross sections of the noble metal *d* levels are almost constant over an energy region from 20 to 1500 eV. This effect was first used by Braun *et al.*² to divide the valence bands into contributions from the noble metal *d* states and chalcogen *p* states in some chalcopyrites. In these experiments no continuous light source was available, only discontinuous gas discharge lamps and x-ray tubes (21.2 eV, 40.8 eV and 1486.6 eV) were used to follow intensity changes in the emission features of the valence band. The valence band decomposition was deduced by a subtracting spectra taken at different photon energies. Since not all of the required cross sections were available at that time, estimates had to be made instead. More recently an investigation of the valence states of CuInSe₂ by tuning the photon energy at a synchrotron radi-

ation source was reported by Takarabe and coworkers.⁷ They point out that the density of Cu *d* states is directly mapped by taking valence band spectra at photon energies above 60 eV. They assigned the observed emissions as bonding, antibonding and non-bonding Cu 3d states following the generic band diagram given by Jaffe and Zunger.¹ However, no quantitative analysis of the relative Cu *d* contribution compared to that of Se *p* states at critical points in the valence bands was given. The aim of this study is to make use of the drastic relative changes in atomic photoionization cross sections of the contributing atomic levels in the valence region at photon energies between 30 and 60 eV to map the relative contributions of Cu 3d and Se 4p states in the valence bands by a fitting procedure that has only a small number of fitting parameters.

II. EXPERIMENT

The experiments were performed at the TGM 7 beamline at the BESSY synchrotron radiation source in Berlin, Germany. A commercial VG analyser chamber (base pressure 3×10^{-11} mbar) equipped with an angular resolving spectrometer (ADES 500) was connected to this beamline. The combined resolution of the monochromator and the spectrometer is approximately $\Delta E/E = 1/300$.

The CuInSe₂ crystals were grown by chemical vapor transport. The as-grown crystals were oriented parallel to the (011) direction by x-ray diffraction, cut into pieces and notched. Then they were fixed to the Cu-sample holders with conducting silver epoxy glue. The crystals were cleaved in the preparation chamber at a pressure of 1×10^{-10} mbar and immediately transferred to the analyser chamber. The surface structures were checked with a (VG) three grid low-energy electron diffraction (LEED) optic. The crystals could only be cleaved along the (011) planes, which is a known cleavage plane of chalcopyrites.^{8,9} In contrast to our experience the (110) plane (known as typical cleavage planes of zinc blende compounds) and the polar (112) plane have also been claimed to be cleavage plane of CuInSe₂.^{10,11} The LEED pattern of the cleaved (011) surface is a rectangular centered array of sharp spots, showing an *a:b* ratio of 1:2.25 which is to be expected for the unreconstructed (011) plane.

Unfortunately, none of the directions for which band structure calculations has been performed, i.e., $\Gamma \rightarrow T$ or $\langle 001 \rangle$ and $\Gamma \rightarrow N$ or $\langle 110 \rangle$,¹ are parallel to the surfaces in-

^{a)} Author to whom correspondence should be addressed; electronic mail: Jaegermann@hmi.de

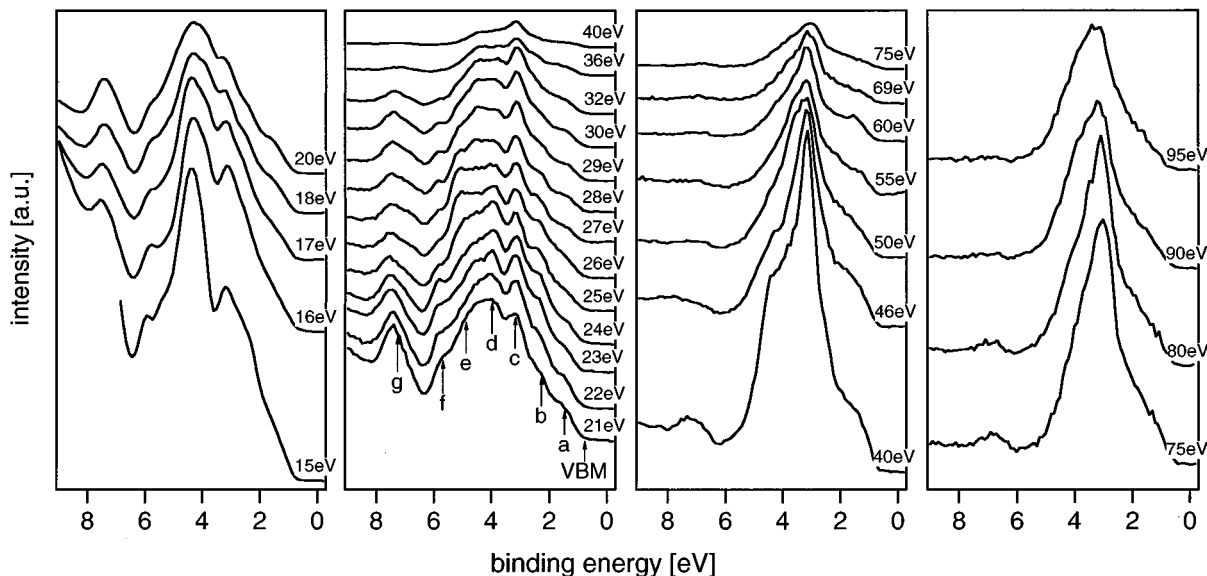


FIG. 1. Valence band spectra taken with excitation energies between 15 and 95 eV. Due to the changes of photoionization cross sections emissions from Se 4p derived states are dominant in the lower photon energy regime. They fade out at excitation energies above 30 eV. The remaining emissions at excitation energies above 60 eV are almost exclusively attributed to Cu 3d.

vestigated. Therefore band structure calculations cannot be directly compared to experimental band mappings at this surface, which could be done in the directions $\Gamma \rightarrow X$ or $\langle 100 \rangle$. Thus we restricted our intensity analysis to valence band states in normal emission.

III. RESULTS AND DISCUSSION

Figure 1 shows a series of photoelectron spectra taken at different excitation energies between 15 and 95 eV. The spectra are depicted as measured, i.e., the small but finite distance between the zero of binding energy scale (Fermi level) and the onset of photoemission (valence band maximum) reflect the p-type conductivity of the sample. Moreover, the spectra are normalized with respect to the incident photon flux, determined from the photocurrent of the exit mirror of the monochromator; due to the decreasing analyser transmission for electrons with higher kinetic energy the count rates of the spectra decrease with higher photon energy. Our spectra show more valence band features (labelled a,b,c...) compared to previously published results.⁷ A detailed comparison of detected peaks in CuInSe₂ valence bands is given in Table I. The assignment of structures is given according to the band structure¹ and according to our experimental results (see below). It is supported by the changes in the emission intensity with the variation of photon energy.

In Fig. 2(a) the calculated photoionization cross sections of Se 4p and Cu 3d valence states and of In 4d core states for photon energies below 100 eV are shown.⁶ It is evident that the spectral features (compare Fig. 1) for excitation energies below 20 eV are dominated by contributions from Se 4p states. Between 20 and 30 eV emissions from Cu 3d and Se 4p contribute about same extent to the electron distribution curve. Above 30 eV the emission intensities from Se states fade out; the remaining emission spectra obtained with exci-

tation energies above 60 eV mostly reflect the Cu 3d contributions to the valence band density of states.

Spectra of the In 4d core level, which due to its high binding energy does not hybridize to the valence band states, were also measured at excitation energies above 25 eV. The In 4d count rate as function of the photon energy can be directly compared with its respective cross section curve. After background subtraction the peak intensities at different excitation energies are theoretically described by²

$$I(h\nu) = A \cdot L(h\nu - E_b) \cdot T(h\nu - E_b) \cdot \sigma_{\text{In } 4d}(h\nu), \quad (1)$$

where A is a spectrometer dependent normalization constant; L is the escape depth of photoelectrons and T the spectrometer transmission function both of which are dependent on the kinetic energy of the photoelectrons; $\sigma_{\text{In } 4d}$ is the photoexcitation cross section. The possible effects of photoelectron diffraction¹² were neglected in Eq. (1). The photon energy range and hence the kinetic energy of the outgoing

TABLE I. Resolved peaks in the valence band of CuInSe₂ excited with $h\nu=21$ eV. Binding energies (BE) are given with respect to the valence band maximum. According to Ref. 7 the peak labelled c is attributed to the non-bonding Cu 3d states, peaks d-f are mainly Se 4p emissions, and g is from the In-Se band.

This work	BE / eV	Ref. 7	BE / eV
a	0.7		
b	1.5	S ₁	1.21
c	2.4	S ₂	1.95
d	3.2	S ₃	2.55
e	4.1	S ₄	3.35
f	4.9		
g	6.5	S ₅	6.6

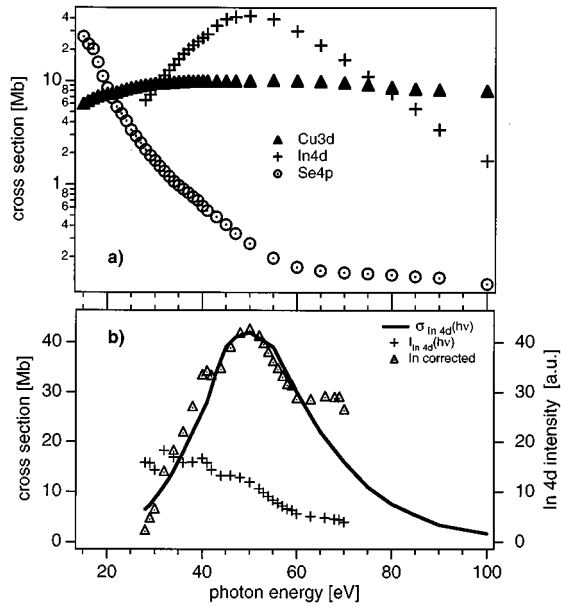


FIG. 2. (a) Variation of atomic photoionization cross sections of Cu 3d, Se 4p, and In 4d levels with excitation energy as given in Ref. 6. (b) Comparison of the In 4d intensity $I_{\text{In } 4d}$ with the In 4d cross section $\sigma_{\text{In } 4d}(h\nu)$. After correction by the analyser transmission function and an appropriate normalization factor reasonable agreement is achieved. The corrected intensity behavior vs photon energy is given by $I_{\text{In } 4d}(h\nu) \cdot 0.16 \cdot (h\nu - 27 \text{ eV})$.

electrons is rather limited, therefore it is reasonable to assume a constant escape depth. Then (1) reduces to

$$I(h\nu) = A \cdot T(h\nu - E_b) \cdot \sigma_{\text{In } 4d}(h\nu). \quad (2)$$

The transmission function of the analyser is approximated as being inversely proportional to the electron kinetic energy $(h\nu - E_b)$.¹³ However, the binding energies of atomic levels given in Ref. 6 differ considerably from experimental values. We therefore corrected the kinetic energy term by adding a constant, yielding $T \propto (h\nu - E_b + C)^{-1}$. After multiplying the In 4d peak intensity by the kinetic energy of the photoelectrons and an appropriate normalization constant we get a reasonable resemblance of this curve with the photoemission cross section (Fig. 2(b)). The deviation of the experimental In 4d intensity curve from the cross section curve σ is less than 10% and may reflect photoelectron diffraction effects, that seem to show up mainly at photon energies above 60 eV.

In the upper valence band region, however, all emissions are distinct superpositions of emissions from Se 4p and Cu 3d levels. In principle, band dispersion,¹⁴ resonance,¹⁵ and diffraction effects,¹² also must be considered in evaluating the intensity of valence band photoemission lines. In order to minimize these effects the analysis was restricted to the energy range between 28 and 60 eV, which gives the strongest relative cross sectional variation and lies outside the range of strong band dispersion (compare Fig. 1) and of Cu 3p-3d resonance. We also checked for p-d resonance enhancement of the valence band features. However, no clear effect could be identified (compare Fig. 1). The diffraction effects are also considered to be small in this low kinetic energy range due to the reduced coherence of valence state photoelectrons

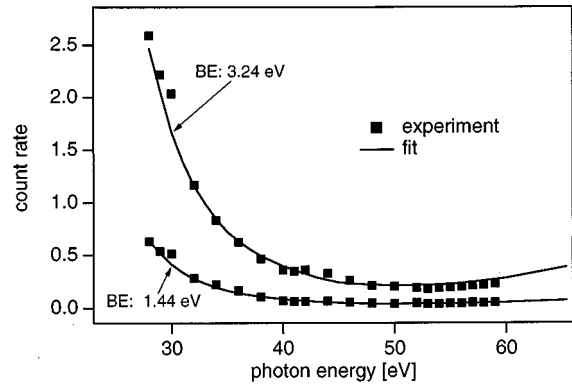


FIG. 3. Count rates in two energy channels (binding energies 1.44 eV and 3.24 eV) vs excitation energies. The course of the count rate is fitted to $N(E, h\nu)$ derived from Eq. (5). At a given energy E the only fit parameters are the densities of states of $\rho_{\text{Cu}}(E)$ and $\rho_{\text{Se}}(E)$.

(no point source). With these approximations the photoemission count rate at any binding energy in the valence band is²

$$N(E, h\nu) = A \cdot T(h\nu - E) \cdot \left(\sum_i \frac{\sigma_i(h\nu)}{n_i} \rho_i(E) \right). \quad (3)$$

By summing the electron densities over the hole valence band the last term will yield the total of valence electrons contributed by Cu 3d and Se 4p atomic electrons:

$$\int_{V_b} \rho_{\text{Cu}}(E) dE = 10 \quad \text{and} \quad (4)$$

$$\int_{V_b} \rho_{\text{Se}}(E) dE = 12$$

(note that there are two Se atoms in every formula unit of CuInSe_2).

The ansatz for the transmission function T is described above. The constant C is inferred from the fit of In 4d to its cross section curve $\sigma_{\text{In } 4d}$ (Fig. 2(b)). In Eqs. (2) and (3) term A still appears and accounts for the spectrometer normalization constant. To reduce fitting parameters we take the ratio of Eqs. (2) and (3) to cancel A . Finally, the count rate of valence band emissions relative to In 4d emission as function of photon energy is given by

$$N(E, h\nu) = \left(\frac{\sigma_{\text{Cu}}(h\nu)}{10} \cdot \rho_{\text{Cu}}(E) + \frac{\sigma_{\text{Se}}(h\nu)}{6} \cdot \rho_{\text{Se}}(E) \right) / \sigma_{\text{In } 4d}(h\nu). \quad (5)$$

The remaining unknown parameters are the respective densities of states $\rho_i(E)$ if known photoionization cross sections, as e.g., those given in Ref. 6, can be applied.

Since the functions $\rho_{\text{Cu}}(h\nu)$ and $\rho_{\text{Se}}(h\nu)$ differ considerably in the photon energy range investigated, we can fit Eq. (5) to the experimentally determined variation of the count rate at a given binding energy as a function of photon energy. Two examples of binding energies 1.44 and 3.24 eV are given in Fig. 3. The experimental curves show some small oscillations around the fitted lines. These are most likely related to the used approximations as, e.g., neglecting

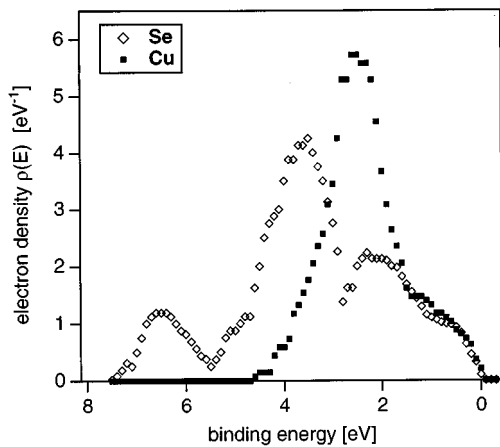


FIG. 4. Densities of states of Cu 3d and Se 4p per formula unit of CuInSe_2 . The contribution of Cu 3d states in the upper part of the valence band is determined to be 50%.

photoelectron diffraction. However, the overall agreement between experimental and calculated values is surprisingly good, considering that only two parameters (ρ_{Cu} and ρ_{Se}) are used for fitting to 22 experimental points in the photon energy range $h\nu=28\text{--}60$ eV. The fitting procedure was applied to each energy channel ($\Delta E=0.1$ eV) of the valence band energy distribution curve (EDC). This yields a set of ρ_{Cu} and ρ_{Se} parameters connected to each binding energy in the valence band that reflect the shape of the respective density of states. In order to obtain the quantitative density of states per formula unit the parameter sets are normalized such as to yield the total of valence electrons according to Eq. (4). The final result of this procedure is presented in Fig. 4.

We can read directly from this graph the contribution of d and p electrons at the respective energy channel. In the binding energy regime between the valence band maximum E_V and the binding energy of 0.8 eV below E_V the mean Cu 3d contribution to the valence band states varies to be $50 \pm 8\%$ (see Fig. 4). The maximum contribution of Cu 3d electrons to the valence band density of states amounts to 75% around 2.4 eV below the valence band maximum. It corresponds to non-bonding d states and is visible as the strongest emission in the spectra with $h\nu \geq 40$ eV and as structure c in the spectrum taken with $h\nu=21$ eV (see Fig. 1). It is important to note that the shape of the Cu 3d density of state distribution determined by our procedure is in very good agreement with the spectra measured at photon energies above 60 eV (which are dominated by the Cu 3d states). The close correspondence of these two independent results is an additional experimental proof of the validity of the procedure applied.

Our determination of the contribution of Cu 3d states in the upper part of the valence band of CuInSe_2 agrees qualitatively with the result of Braun *et al.*² obtained for CuInS_2 (60% Cu 3d character). There is evidently a strong hybridization of the Cu 3d states with the Se 4p states in the valence band that is evidently underestimated in the band structure calculations.^{1,16}

There may be a systematic uncertainty in the applied procedure due to the use of atomic photoionization cross

sections in Eq. (5). It has been shown experimentally that significant changes of σ may occur especially for 4d metals close to the Cooper minimum¹⁷ when different environments—atoms, bulk metals, or compounds—are compared.^{18,19} In principle, it cannot be excluded that the photoionization cross sections of Cu and Se in CuInSe_2 are also different from their atomic values. But a pronounced Cooper minimum is not reported for Se and Cu 3d states which show only a smooth variation of σ with $h\nu$.⁶ In addition, the strongest variations in σ were reported when atoms are compared to delocalized metallic states.^{18,19} For rather localized states in covalent compounds, a reasonable agreement of σ with atomic values is reported.^{18,20,21} We therefore assume that atomic photoionization cross sections can be applied as a reasonable approximation for excitation processes involving the rather localized states of the CuInSe_2 valence band.

IV. SUMMARY

We have measured the valence band of $\text{CuInSe}_2(011)$ cleavage planes using photoelectron spectroscopy with varying excitation energy. The spectral features can be assigned by using the energy dependence of photoionization cross sections. In addition, the relative intensities are evaluated using the In 4d core line as a reference to extract the Cu 3d and Se 4p contributions to the partial density of states in the valence band. Future investigations are planned to analyse the valence band spectra of the chalcopyrite family to systematically deduce the role of group I-d/ group VI-p hybridization of the electronic structure.

- ¹J. E. Jaffe and A. Zunger, Phys. Rev. B **28**, 5822 (1983).
- ²W. Braun, A. Goldmann, and M. Cardona, Phys. Rev. B **10**, 5069 (1974).
- ³J. L. Shay and J. H. Wernick, *Ternary Chalcopyrite Semiconductors*, (Pergamon, Oxford, 1975).
- ⁴H. Sommer, A. Weiss, and H. Neumann, Phys. Status Solidi A **162**, K87 (1990).
- ⁵H. Sommer, A. Weiss, H. Neumann, and R. D. Tomlinson, Cryst. Res. Technol. **25**, 1183 (1990).
- ⁶J. J. Yeh and I. Lindau, At. Data Nucl. Data Tables **32**, 2 (1985).
- ⁷K. Takarabe, K. Kawai, and S. Minomura, J. Appl. Phys. **71**, 441 (1992).
- ⁸M. Sander, M. Jaegermann, and H. J. Lewerenz, J. Phys. Chem. **96**, 782 (1992).
- ⁹W. Jaegermann, T. Löher, and C. Pettenkofer, Cryst. Res. Technol. **31**, 273 (1996).
- ¹⁰T. P. Massopust, P. J. Ireland, and L. L. Kazmerski, J. Vac. Sci. Technol. A **2**, 1123 (1984).
- ¹¹F. A. Abou-Elfotouh, L. L. Kazmerski, H. R. Moutinho, J. M. Wissel, R. G. Dhere, A. J. Nelson, and A. M. Bakry, J. Vac. Sci. Technol. A **9**, 554 (1991).
- ¹²C. S. Fadley, Prog. Surf. Sci. **16**, 275 (1984).
- ¹³D. Briggs and M. P. Seah, *Practical Surface Analysis by Auger and X-Ray Photoelectron Spectroscopy* (Wiley, New York, 1983).
- ¹⁴F. J. Himpsel, Adv. Phys. **32**, 1 (1983).
- ¹⁵M. R. Thuler, R. L. Benbow, and Z. Hurych, Phys. Rev. B **26**, 669 (1982).
- ¹⁶P. Bendt and A. Zunger, Phys. Rev. B **26**, 3114 (1982).
- ¹⁷J. W. Cooper, Phys. Rev. **128**, 681 (1962).
- ¹⁸G. Rossi, I. Lindau, L. Braicovich, and I. Abbati, Phys. Rev. B **28**, 3031 (1983).
- ¹⁹R. J. Cole, J. A. Evans, L. Duo, A. D. Laine, P. S. Fowler, P. Weightman, G. Mandio, and D. Norman, Phys. Rev. B **46**, 3747 (1992).
- ²⁰I. Abbati, L. Braicovich, C. Carbone, J. Nogami, J. J. Yeh, I. Lindau, and U. del Pennino, Phys. Rev. B **32**, 5459 (1985).
- ²¹G. N. Kwawer, T. J. Miller, M. G. Mason, Y. Tan, F. C. Brown, and Y. Ma, Phys. Rev. B **39**, 1471 (1989).